Locomotion Control of *Caenorhabditis elegans* through Confinement

Félix Lebois,[†] Pascal Sauvage,[†] Charlotte Py,[†] Olivier Cardoso,[†] Benoît Ladoux,[†‡] Pascal Hersen,[†‡] and Jean-Marc Di Meglio[†*]

[†]Matière et Systèmes Complexes, UMR 7057, Centre National de la Recherche Scientifique and Université Paris Diderot, Paris, France; and [‡]Mechanobiology Institute, National University of Singapore, Singapore

ABSTRACT The model organism *Caenorhabditis elegans* shows two distinct locomotion patterns in laboratory situations: it swims in low viscosity liquids and it crawls on the surface of an agar gel. This provides a unique opportunity to discern the respective roles of mechanosensation (perception and proprioception) and mechanics in the regulation of locomotion and in the gait selection. Using an original device, we present what to our knowledge are new experiments where the confinement of a worm between a glass plate and a soft agar gel is controlled while recording the worm's motion. We observed that the worm continuously varied its locomotion characteristics from free swimming to slow crawling with increasing confinement so that it was not possible to discriminate between two distinct intrinsic gaits. This unicity of the gait is also proved by the fact that wild-type worms immediately adapted their motion when the imposed confinement was changed with time. We then studied locomotory deficient mutants that also exhibited one single gait and showed that the light touch response was needed for the undulation propagation and that the ciliated sensory neurons participated in the joint selection of motion period and undulation-wave velocity. Our results reveal that the control of maximum curvature, at a sensory or mechanical level, is a key ingredient of the locomotion regulation.

INTRODUCTION

Numerous limbless organisms, from small nematodes (1) to eels (2), use oscillatory body deformations for propulsion; snakes undulate on solid surfaces (3); sandfish lizards even move through granular materials without the aid of their limbs (4). In most cases, forward propulsion is achieved through the backward propagation of a flexural wave generated by muscular contraction (5). The simplicity and the robustness of undulatory locomotion has inspired the design of robotic devices that are able to cope with complex environments (6) and open new possibilities for the propulsion of micro-swimmers for medical applications (7).

The *Caenorhabditis elegans* nematode is a model organism whose main phenotype is locomotion (8). Ventral cord motor neurons innervate two dorsal and two ventral rows of 23 muscular cells that give the worm the ability to locally and periodically deform its elastic cuticle, hence generating flexural waves that propagate from head to tail (for forward locomotion) (9).

C. elegans locomotion is usually observed in two very different experimental situations in research laboratories. Totally immersed worms swim with a characteristic bending frequency of ~2 Hz and exhibit a typical C-shape; on the wet surface of a plane agar gel, *C. elegans* worms crawl, the worm body is pinned on the gel by capillarity with a characteristic S-shape, and the bending frequency is reduced to ~0.5 Hz. It is then interesting to investigate whether these two different locomotory behaviors correspond to two different gaits (as for instance, walking and running for humans) and use the extensive accumulated knowledge of the neural system of the worm to identify different neural command systems.

Another interesting issue, if the existence of two different gaits is proved true, is to understand how a particular gait is selected: is it the result of energy optimization (like for human gaits (10,11)), or is it the response of the neural system of the worm to perception or proprioception sensors? In any case, it should not forgotten that the natural habitat of *C. elegans* is not very well known. The strains studied by biologists were isolated in composts and in garden soils, i.e., moist three-dimensional environments (12) with very different geometries and topologies compared to bulk liquid or planar surfaces: any conclusion drawn from lab experiments involving the adaptation of the worm to its environment should then be made with caution. New studies have recently been published for locomotion in granular media (13,14) that provide a more natural environment for the worm.

Insights into the control of undulations can be provided through mechanical perturbations of *C. elegans* locomotion. A first and simple method is to modify the viscosity of the liquid: Berri et al. (15) recorded the motion of worms in aqueous solutions of gelatin at different concentrations and showed that the frequency, the wavelength, and the amplitude of the flexural wave decreased continuously as the medium becomes non-Newtonian. They concluded that swimming and crawling are modulations of the same

Submitted January 17, 2012, and accepted for publication April 25, 2012.

*Correspondence: jean-marc.dimeglio@univ-paris-diderot.fr

Editor: E. Ostap.

0006-3495/12/06/2791/8 $2.00

doi: 10.1016/j.bpj.2012.04.051

gait. Similarly, Korta et al. (16) studied the effect of increasing the viscosity of the liquid: the worm shape is preserved whereas the frequency decreases by 20% for a 1000-fold increase in viscosity. They further showed that mutations affecting mechanosensation or the killing of touch receptor neurons slightly increased the frequency of the swimming gait, suggesting a modulation through mechanosensory inputs. Fang-Yen et al. (17) also reached the conclusion of a continuously monitored single gait from studies where the viscosity of the liquid medium was changed by addition of polysaccharide and discussed the worm adaptation to the mechanical load.

Recently, Shen and Arratia (18) showed that *C. elegans* could swim in a viscoelastic liquid with a reduced velocity and Sznitman et al. (19) showed that, using Newtonian liquids, that *C. elegans* could be considered as a good model of low Reynolds swimmer. However, Pierce-Shimomura et al. (20) maintained the swimming/crawling partition, evidenced by calcium imaging of the muscular activity and the report of mutants that could not rapidly switch from crawling to swimming (*unc-79*, *unc-80*) or that showed transient crawling-like behavior in liquid (*che-3*). Two articles of the same group by Mesce and Pierce-Shimomura (21) and Vidal-Gadea et al. (22) also showed very recently that these putative two gaits could be selected in particular via dopamine or serotonin. The existence of different gaits and their selection is then not a closed problem (23) and raises exciting issues about decision-making by animals.

In this article, we present what to our knowledge is a totally new experiment where the environment of a single worm can be continuously varied between the common laboratory experimental situations where swimming and crawling is observed. The principle of the experiment is to squeeze a worm between a glass plate and an agar gel (Fig. 1 *a*). When the gap is larger than the worm diameter, the experimental situation corresponds to a worm in bulk liquid, whereas for a gap smaller than the worm diameter, the confinement mimics the situation of petri dishes where the worm is pinned by surface tension and deforms the gel (Fig. 1 *b*).

Our original setup modulates the worm environment in a novel-seeming way with respect to previous studies where the viscoelastic properties of the surrounding fluid are varied: in particular, we can reasonably assume than the mechanical receptors of a squeezed worm are excited in a way similar to that of a worm confined by capillarity. The setup imposes a geometrical confinement and is not equipped to measure the pressure applied on the worm. Nevertheless, an estimate of this pressure could be derived as follows (24). For small deformations of the gel, the elastic stress σ is given by

$$\sigma \simeq E\frac{h}{\sqrt{Rh}} \sim E\epsilon^{1/2}, \qquad (1)$$

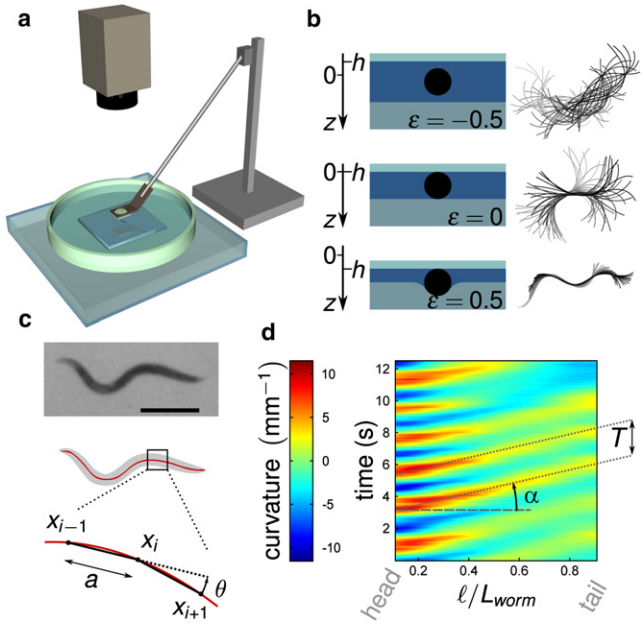

FIGURE 1 Experimental framework. (*a*) Setup. A worm is confined between an agar gel and a glass plate that can be moved vertically. Movies are recorded with a charge-coupled device camera through a stereo microscope (see Materials and Methods). (*b*) (*Left*) Cross sections of the confined worm, for different values of ϵ; (*right*) corresponding superpositions of the worm midline over 2 s. (*c*) Image analysis. (*Top*) Raw image (scale bar 0.5 mm); (*center*) thresholded image (*gray*) and skeletonization (*red line*); (*bottom*) the body curvature is computed as $\kappa = \theta/a$. (*d*) Spatiotemporal plots of the curvature versus a nondimensional curvilinear coordinate from head to tail (ℓ/L_{worm}).

with E the Young modulus of the gel, R the worm radius, h the indentation depth of the gel, and $\epsilon = h/(2R)$ the relative confinement (see Materials and Methods). $E \simeq 5.10^5$ Pa (25) for a 2% gel, we could then apply a confinement pressure between 0 and 10^5 Pa on the worm. This has to be compared to the situation where the worm is pinned by capillarity on an agar gel (the confinement pressure can be estimated by $\gamma/R \simeq 10^3$ Pa with γ the surface tension of the wetting film on the gel) and to the situation of a worm in bulk liquid where the hydrodynamic stress is given by $\eta V/R$ (with η the liquid viscosity and V a characteristic velocity of the worm): increasing the viscosity of the surrounding liquid by polymer addition was used to vary the viscous stress between 0.01 and 100 Pa (17). Our setup then allows us to investigate conditions that encompass most lab conditions experienced by the worm, and beyond.

MATERIALS AND METHODS

Strains

Wild-type (WT) *C. elegans* (N2), and the mutant strains *mec-4*(*e1611*), *unc-79*(*e1068*), *trp-4*(*sy695*) and *che-3*(*e1124*) were obtained from the *C. elegans* Genetics Center (Minneapolis, MN). Worms were grown at 16°C on nematode growth media plates seeded with *Escherichia coli*

OP50. A standard small-scale synchronization procedure (26) was used to obtain young adults: worms were imaged 96 h after the transfer of starved L1 to a fresh plate with food. They were then washed in M9 buffer before being transferred to the acquisition setup.

Experimental setup

To observe the transition from swimming to crawling, a single worm was placed into M9 liquid buffer and gradually confined between a glass plate and the surface of a planar, soft, deformable aqueous gel (2% agar gel) (Fig. 1 *a*). The glass plate and its support were held by a rod whose vertical position was controlled with a motorized linear actuator coupled to a motion controller (NSA12 and NSC200; Newport, Irvine, CA), operated with LabVIEW (National Instruments, Austin, TX). The vertical position of the glass plate was controlled with an accuracy of <1 μm. The gel was prepared as follows: an agar solution heated above the gel temperature (~35°C) was poured in a large petri dish (110-mm diameter); a large glass plate was fixed on the confinement upper plate and put in contact with the agar solution. This large plate was removed after the gelation of the agar solution occurred on cooling. This process ensured a perfect parallelism of the two confinement surfaces of the setup. To maintain a constant temperature of the bath of 20°C, the setup was placed upon a transparent cell through which temperature-controlled water flowed. The whole was placed under a stereo microscope (SZX10; Olympus, Tokyo, Japan) and observations were made in transmitted light. We observed one single worm at a time. The worm motion was recorded through the microscope at 18 frames/s using a charge-coupled device camera (PL-B741F, 1280×1024 resolution; PixeLINK, Ottawa, Ontario, Canada). This acquisition frequency was sufficient to capture the worm essential features. At each position of the glass plate, 30–60 s-long movies were acquired. Observation of a single worm lasted no more than 30 min, to avoid episodes of quiescence (27) or effects of exhaustion. Approximately 12 worms were submitted to confinements ranging from $\epsilon = -0.8$ to $\epsilon = 1$ for each strain (see next paragraph for the definition of the confinement parameter ϵ and Section S1 in the Supporting Material for a description of the data analysis).

Confinement parameter ϵ

After insertion of a new individual inside the setup, the glass plate was lowered down until the worm touched both the plate and the gel; this defined the reference position $h = 0$ that was easily detected from the immobilization of the center of the worm (see the superposition of the midlines of the worm, Fig. 1 *b*, *center*); the gap distance between the gel and the glass plate was then equal to $2R$ with R the maximum radius of the worm at its center (*C. elegans* can be considered as a cylinder with tapered ends; $2R$ was measured using an optical microscope). The glass plate vertical position h was counted algebraically from this reference position, so to have positive values of h for smaller gaps, negative values otherwise. The nondimensional confinement parameter ϵ is defined as $\epsilon = h/(2R)$. Positive values of h thus corresponded to situations where the gel was indented by the worm ($\epsilon = 1$ was the situation where the gel is in full contact with the upper glass plate), whereas negative values described situations where the worm touched neither the plate nor the gel. Interestingly, in this latter situation and for the studied confinements ($\epsilon > -1$), the trajectory of the worm was directed by the walls and remained planar, in the focusing plane of the microscope.

A typical experiment was run as follows: we first sought the position $h = 0$ as described above and the upper plate was then displaced to obtain the desired confinement ϵ. The trajectory of the worm was recorded and the worm was then released by shifting up the upper plate. This protocol was repeated for a range of confinement parameters. We also studied experimental situations in which initially squeezed worms ($\epsilon = 0.41$) were progressively released, for two different release rates: $d\epsilon/dt = -0.07$ (slow release) or 0.7 s^{-1} (fast release); see Fig. 4.

Image processing

Movies of the worm were analyzed using an image processing software (ImageJ; National Institutes of Health, Bethesda, MD (28)). After background correction, the images were smoothed and thresholded (Fig. 1 *c*). The worm body was reduced to a single continuous line using the "skeletonize" function of ImageJ. The coordinates of the midline of the worm were then saved for subsequent motion analysis. The determination of the motion characteristics was done with GNU Octave (29), following a similar approach to previous studies (15,16). For each video frame, the body coordinates were first fitted with a cubic smoothing spline with 100 points evenly distributed along the length of the worm. The curvature of the body at a given point $\mathbf{x_i}$ was computed from the angle between the vectors ($\mathbf{x_{i+1}} - \mathbf{x_i}$) and ($\mathbf{x_i}$ and $\mathbf{x_{i-1}}$). Curvature was plotted against time and curvilinear nondimensional coordinate ℓ/L_{worm} to highlight its propagation along the worm body from head to tail (Fig. 1 *d*) (ℓ is the curvilinear abscissa taken from the head and L_{worm} is the length of the worm).

The accuracy of the determination of the curvature at the extremities was very low so that we limited the spatiotemporal graphs to $0.1 \leq \ell/L_{worm} \leq 0.9$. Linear fits of the oblique red-yellow (positive curvature) and blue (negative curvature) stripes on the spatiotemporal graph were used to measure the period of motion, T, and the phase velocity of the curvature, V_w (Fig. 1 *d*): all reported results are averages obtained with a collection of 12 individual worms. For the sake of illustration of the variability of the worm behaviors, Fig. S1 in the Supporting Material compares, for WT worms, the dependence of the period T and the wave velocity V_w on the confinement of four individual worms (among the studied population of 12 worms) with the average dependence of the studied population. These dependences are identical within the error bars and then do not depend on worm sampling: this proves the robustness of the worm behaviors versus confinement. The worm displacement velocity V was measured as the velocity of its centroid in the main direction of the motion averaged over 20 frames.

RESULTS AND DISCUSSION

Wild-type worms

To begin, we investigated the behavior of wild-type (WT) worms (N2 strains) when the confinement gap was gradually reduced (see Movie S1 in the Supporting Material) in a quasistatic way. As long as the worm did not touch the glass plate and the gel ($\epsilon < 0$), the period T and the wave velocity V_w remained constant (Fig. 2, *a* and *b*), and the worms exhibited the typical C-shape of a swimming worm in liquid (Fig. 2 *e*). The swimming velocity increase on approaching $\epsilon = 0$ (Fig. 2 *d*) can be ascribed to a purely hydrodynamical effect: the transverse friction coefficient increases faster than the longitudinal friction coefficient as the gap narrows (see Section S3 in the Supporting Material).

For $\epsilon = 0$, the worm touched both the glass plate and the gel at its center (wider part of its body) while its head and tail could still oscillate; in this particular situation, the friction forces generated by the motions of the body in the liquid were smaller than the friction force between the worm and the gel, and the worm could barely move forward. The body shape then gradually turned into a S-shape as ϵ increased (Fig. 2 *e*), adopting a similar shape to what it would be on an agar gel in a petri dish, a situation corresponding to $\epsilon \simeq 0.4$ (see Section S4 in the Supporting

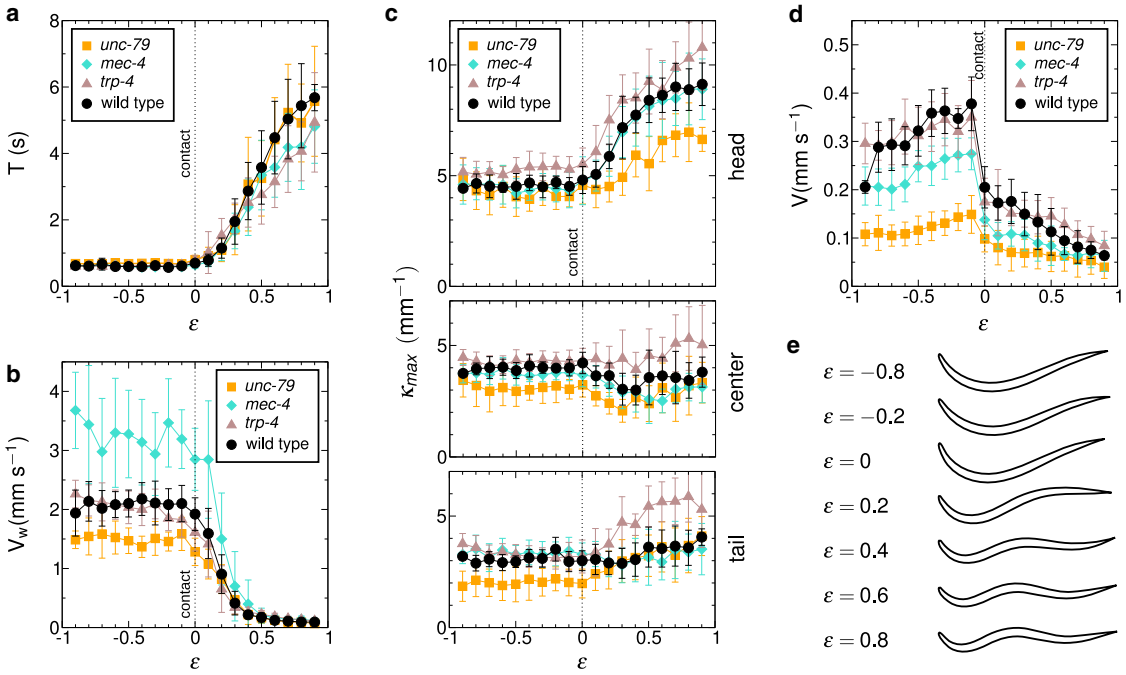

FIGURE 2 Evolution of the kinematic parameters with confinement for WT and mutant worms. (*a*) Period. For *mec-4* and *unc-79* mutants only the period of head oscillations is measured, as these oscillations do not correctly propagate along the body. (*b*) Propagation velocity. (*c*) Maximum curvature for the head region (*top*), at midbody (*center*) and for the tail (*bottom*). (*d*) Displacement velocity. (*e*) The weighted average of the first four *eigenworms* reflects the continuous transition in the space of shapes for WT worms.

Material). Both the period T and the wave velocity V_w evolved continuously with the confinement, T showing a 10-fold increase whereas V_w dropped from 3 to 0.1 mm.s^{-1} (Fig. 2, *a* and *b*).

The maximum curvature measured at different parts of the body remained very much constant, with the exception of the head, the oscillations of which became larger as the confinement was increased (Fig. 2 *c*). This conservation of curvature was also observed in the episodes of backward locomotion (see Fig. S2). We emphasize that in the crawling regimes, the friction experienced by the worm is much greater than the friction in liquid and the difference between longitudinal and transverse friction coefficients is drastically enhanced, as shown in a previous study (24).

Another set of experiments investigating the behavior of worms confined in a channel revealed the robustness of the conservation of the maximal curvature. A single WT worm was placed on an agar gel between two rigid walls (made out of cured SU8 photoresist, see Fig. 3 *a*), delimiting a channel. Capillary forces confined the worm inside this channel. The width of the channel could be modified, thus restricting the amplitude A of the movement to half of the channel width. Values of the wavelength λ were measured for ~10 individuals placed in channels of variable width or allowed to crawl on agar without walls. The wavelength λ was found to decrease with the width of the channel, as shown in Fig. 3 *b*. A very simple model can enlighten these observations. For the sake of simplicity, we consider the radius λ of the worm negligible compared to the width of the channel. The maximal curvature (in absolute value) is then given by

$$C_{max} \sim \frac{A}{\lambda^2}. \tag{2}$$

If the maximal curvature is an invariant of the locomotion, we should have

$$\lambda \sim A^{1/2}. \tag{3}$$

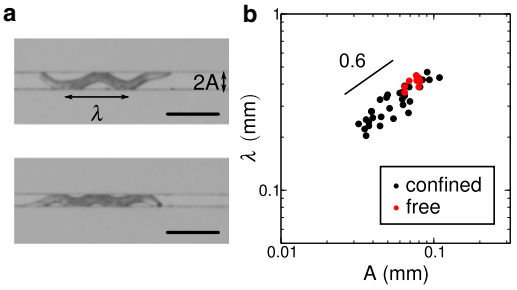

FIGURE 3 Crawling between rigid walls. (*a*) A single WT worm is allowed to crawl between two rigid walls; the gap between the walls can be modified. The photographs correspond to two values of the channel width: 0.09 mm (*top*) and 0.06 mm (*bottom*). The width of the channel constrains the amplitude A of the movement, and consequently the wavelength λ. Scale bar represents 0.25 mm. (*b*) Evolution of the wavelength λ as a function of the amplitude A (logarithmic scale), for confined worms (*black dots*) and for free crawling worms (*red dots*). A linear fit on confined worms' data gives $\lambda \sim A^{0.6}$.

A linear fit on the logarithmic plot of the experimental data (Fig. 3 *b*) gives $\lambda \sim A^{0.6}$, thus compatible with the constancy of the maximal curvature.

The gradual change of shape observed when varying ϵ can be evidenced (Fig. 2 *e*) by using the approach of Stephens et al. (30) to compute the first four eigenworms using principal component analysis (see Section S5 in the Supporting Material). The weighted average of these eigenworms can be considered as a typical but fictitious shape that captured the essential features of the body posture and reflects its continuity in the space of shapes as the degree of confinement is varied.

Our observations did not reveal any discontinuity between the two modes of locomotion for WT worms and therefore support the conclusion of Berri et al. (15) that swimming and crawling are two samples of the same gait modulated by the mechanical environment.

In addition, the response to the confinement modulation occurred progressively, without intermediate posture or adaptation behavior: an initially confined worm at $\epsilon = 0.41$ was released by lifting up the glass plate until $\epsilon = -1$ (Fig. 4, *a* and *b*, and see Movie S2). The spatiotemporal graph shows how the worm constantly adapted its shape and frequency to the decreasing confinement and eventually recovered its swimming pattern. The results obtained when the glass plate was suddenly lifted up are shown in Fig. 4 *c*: the worm instantaneously adapted to the new environment (see Movie S3); "instantaneously" means that no arrest time larger than the acquisition time of the camera (1/18 s) could be distinguished (we also performed experiments at the maximal frame rate of 27 fps with similar results). The existence of a time lag would have been indeed the signature of a switching process in the neuronal processing of the mechanical information and the muscles control. We performed similar experiments in compression (see Fig. S7) that lead to the same observations and conclusions. We did not observe arrest times as reported in Vidal-Gadea et al. (22) for crawling worms suddenly put in water, but this constitutes a very different experimental situation.

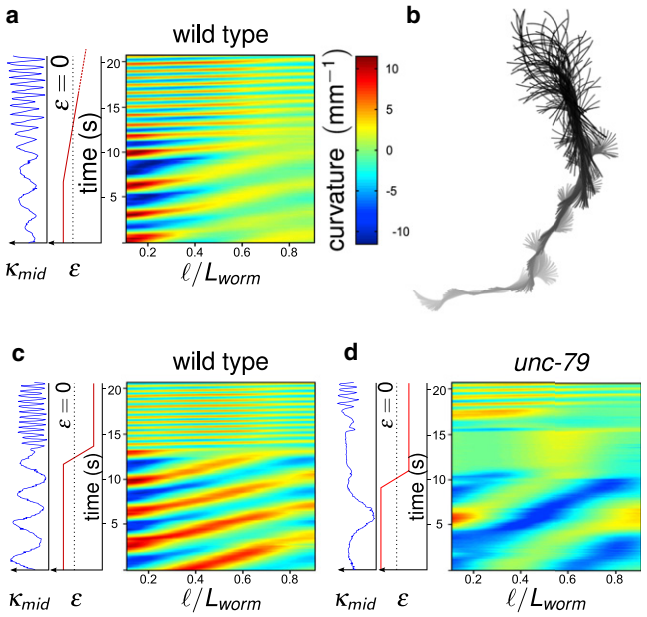

FIGURE 4 Dynamical variation of the confinement parameter ϵ. (*a* and *b*) Spatiotemporal dynamics of a WT individual progressively released ($d\epsilon/dt = -0.07\ s^{-1}$) from its initial confinement ($\epsilon = 0.41$). (*a*) Spatiotemporal graph of the curvature and corresponding evolution of ϵ (*red*) and of the curvature at midbody κ_{mid} (*blue*). (*b*) Projection over time of the successive skeletonized shapes of a WT worm during its release, from crawling (*gray*) to swimming (*black*). (*c* and *d*) Spatiotemporal graphs of the curvature for a sudden release ($d\epsilon/dt = -0.7\ s^{-1}$) for WT (*c*) and *unc-79* mutant (*d*).

Mutant worms

To gain more insight into the regulation of the undulations, we studied mutants with very different locomotion phenotypes: *mec-4*(*e1611*), which is insensitive to light touch (31); *trp-4*, which cannot control its curvature (32); *unc-79*, which exhibits abnormal swimming (33); and *che-3*, which was described as spontaneously switching between swimming and crawling in bulk liquid (20).

mec-4

MEC-4 along with MEC-10 is part of the mechanotransduction complex of the six touch receptor neurons (34,35) and *mec-4* mutants do not respond to light touch. We were expecting a very different behavior from WT worms, especially when the worm was barely in contact with the two confinement surfaces (i.e., when $\epsilon \geq 0$, in a situation corresponding to light touch). When unconfined (i.e., when $\epsilon < 0$), the worm swam slower than WT worms (Fig. 2 *d*), despite a larger wave velocity (Fig. 2 *b*) that should have led to an enhanced velocity according to slender body locomotion models (1) (see Movie S4). The undulations period behaved very much like the period of WT worms (Fig. 2 *a*) but *mec-4* worms also crawled slower than WT worms (Fig. 2 *d*). Although *mec-4* worms could adapt their gait to the confinement, they did it inefficiently probably because of a poor propagation of the curvature wave as evidenced on Fig. 5. When $\epsilon > 0.5$, successive curvature waves might have different velocities and might even fuse before reaching the tail end. The head motions did not seem altered; the locomotion defect introduced by the *mec-4* mutation thus mainly affects the curvature propagation.

Our findings are in contradiction with the results of Korta et al. (16), which showed an increase of the beating frequency of swimming *mec-4* worms (1.8 Hz vs. 1.5 Hz for the WT strain), with a preserved shape. They conversely agreed with observations made with a less severe mutant *mec-4*(*e1339*) (36). Our set of experiments shows that mechanosensation is required for a complete propagation of the bending wave along the worm body. More specifically,

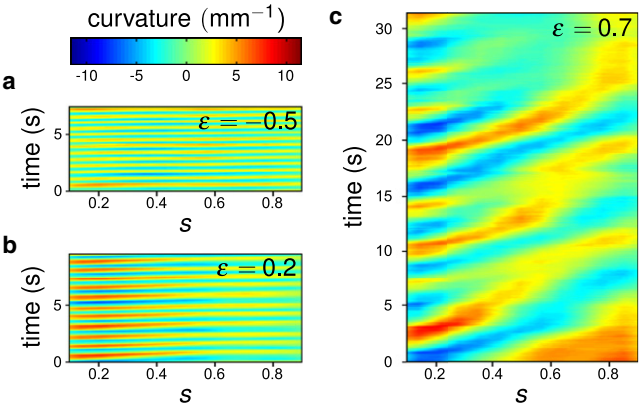

FIGURE 5 Typical spatiotemporal plots of the curvature for *mec-4* for $\epsilon = -0.5$ (*a*), $\epsilon = 0.2$ (*b*), and $\epsilon = 0.7$ (*c*).

because we observe a reduced velocity (as compared to WT worms) even for weak confinement ($\epsilon < 0$), we might suppose that the six light touch receptors participate in the worm proprioception and regulate the worm undulations (because these receptors are attached to the cuticle). Our results also show that the wave velocity of WT worms is not an upper limit and could be overpassed. This might be used by WT worms to get a velocity boost in escape situations, for instance.

trp-4

Another control of the locomotion might be provided by an internal measure of the body response to the combined forces provided by the muscular contraction and the resistance of the environment, namely proprioception. Because the maximal curvature of the body of WT worms remains constant during motion (Fig. 2 *c*), we studied the response of *trp-4*: TRP-4 acts in the stretch-sensitive neuron DVA to regulate the amplitude of body bending during locomotion (32) (it is also present in ciliated neurons such as CEP, ADE, and PDE (37)). The *trp-4* mutants indeed exhibited an increased bending phenotype (higher maximal curvature) for all confinement values (Fig. 2 *c*, and see Movie S5), but their kinematic parameters remained very close to WT ones (Fig. 2, *a*, *b*, and *d*).

unc-79

Fainter mutants such as *unc-79* (see Movie S6) have been described as being unable to switch to swimming when immersed in liquid (20). Our experimental results show that the defective locomotion of swimming *unc-79* worms is due to a slower propagation of the flexural wave (Fig. 2 *b*) and a decrease of its intensity as it reaches the tail, thus explaining the S-shape of swimming mutant worms. Moreover, in contrast with WT worms that adapt their locomotion immediately after release, *unc-79* mutants remained immobile during a short period (5 s on Fig. 4 *d*) before starting to swim. Interestingly, this arrest time is similar to the one observed by Vidal-Gadea et al. (22) but for WT worms. It could be interpreted as the time needed to switch to a different gait but also to the time needed for the initiation of a new undulation wave. Our results confirm that, as hypothesized by Pierce-Shimomura et al. (20), UNC-79 could have a role in the dynamics of the motor neurons involved in the propagation of the curvature.

che-3

Finally, we studied *che-3* worms that are defective in the development of ciliated sensory neurons but conserve the light touch response. These mutants crawl like WT worms on gels (with a smaller velocity) but switch between swimming and crawling-like patterns in liquid (20). We report in Fig. 6 the evolution of the period of the undulations and the wave velocity versus the confinement parameter. Interestingly, we did not observe the bimodal distribution of gaits for unconfined worms as noticed in Pierce-Shimomura et al. (20) and the (T, V_w) values did not seem to correlate with the confinement ϵ. Nevertheless, it is remarkable that the WT provides a lower bound for the period T (Fig. 6 *a*) and an upper bound for the wave velocity V_w (Fig. 6 *b*); these two bounds nevertheless do not represent the mechanical limits of the worm because the V_w bound is overpassed by *mec-4*. This suggests that the function assumed by the ciliated sensory neurons is necessary to determine the worm locomotion pattern that is thus not only determined by the mechanical environment of the worm.

Even though we could distinguish in our experiments the different locomotion phenotypes, the mutants showed the same behavior with respect to confinement experiments (except for *che-3* worms, which do not adapt to their environment). Importantly, with the exception of the head, the maximal curvature for a given part of the body was constant in the various explored environments (Fig. 2 *c*). This does not originate from a physiological limit: for instance, WT worms move backward with enhanced body curvature (see Fig. S2). The control of curvature is thus a key ingredient of the modulation of the locomotion in *C. elegans*, at a neural level using mechanical receptors (38) or at a mechanical level (39).

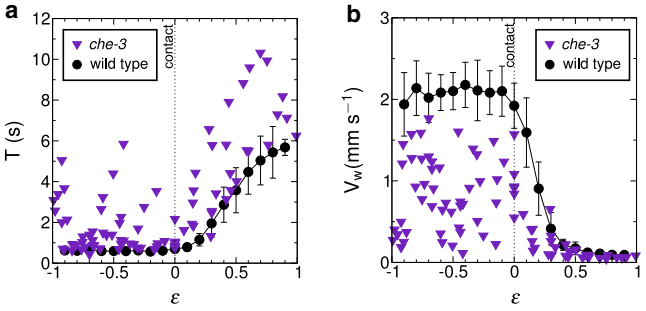

FIGURE 6 Locomotion of *che-3* as a function of confinement. Measurements collected on five different worms along with the average behavior of WT worms for sake of comparison: period (*a*), wave velocity (*b*).

CONCLUSION

In this article, we report what to our knowledge are new experimental results where the mechanical environment of the nematode *C. elegans* is varied by confining a single worm between a glass plate and a planar agar gel. An interesting feature of our experimental setup was the opportunity to dynamically change the confinement while directly recording the worm response. We found that WT worms are able to continuously adapt their locomotion pattern to the confinement geometry, which would imply that WT worms have a single gait. We also found that the light touch response is necessary to a proper propagation of the curvature waves along the worm body. An important result of our study is that the control of curvature might be an intrinsic feature of undulation locomotion. Our data should be confronted with existing models of *C. elegans* locomotion that rely on such feedback mechanisms (40–42) and to experiments with other undulating animals.

SUPPORTING MATERIAL

Seven figures, one table, and six movies are available at http://www.biophysj.org/biophysj/supplemental/S0006-3495(12)00551-6.

The authors thank Dr. Jean-Louis Bessereau (Ecole Normale Supérieure, Paris) for illuminating discussions and advice and Prof. Tim Senden (Australian National University, Canberra) for a critical reading of the manuscript.

This work was supported by the Agence Nationale de la Recherche ("Locomelegans" NT05-3-41923).

REFERENCES

1. Gray, J., and H. W. Lissmann. 1964. The locomotion of nematodes. *J. Exp. Biol.* 41:135–154.
2. Gillis, G. B. 1998. Neuromuscular control of anguilliform locomotion: patterns of red and white muscle activity during swimming in the American eel *Anguilla rostrata*. *J. Exp. Biol.* 201:3245–3256.
3. Gray, J. 1946. The mechanism of locomotion in snakes. *J. Exp. Biol.* 23:101–120.
4. Maladen, R. D., Y. Ding, …, D. I. Goldman. 2009. Undulatory swimming in sand: subsurface locomotion of the sandfish lizard. *Science.* 325:314–318.
5. Gray, J. 1953. Undulatory propulsion. *Q. J. Microsc. Sci.* 94:551–578.
6. Crespi, A., A. Badertscher, and A. Guignard. 2005. AmphiBot I: an amphibious snake-like robot. *Robot. Auton. Syst.* 50:163–175.
7. Dreyfus, R., J. Baudry, …, J. Bibette. 2005. Microscopic artificial swimmers. *Nature.* 437:862–865.
8. Brenner, S. 1974. The genetics of *Caenorhabditis elegans*. *Genetics.* 77:71–94.
9. Von Stetina, S. E., M. Treinin, and D. M. Miller, 3rd. 2006. The motor circuit. *Int. Rev. Neurobiol.* 69:125–167.
10. Alexander, R. M. 2002. Principles of Animal Locomotion. Princeton University Press, Princeton, NJ.
11. Diedrich, F. J., and W. H. Warren, Jr. 1995. Why change gaits? Dynamics of the walk-run transition. *J. Exp. Psychol. Hum. Percept. Perform.* 21:183–202.
12. Kiontke, K., and W. Sudhaus. 2006. Ecology of *Caenorhabditis* species. *In* WormBook. The *C. elegans* Research Community. WormBook, doi/10.1895/wormbook.1.37.1, http://www.wormbook.org.
13. Juarez, G., K. Lu, …, P. E. Arratia. 2010. Motility of small nematodes in wet granular media. *Europhys. Lett.* 92:44002.
14. Jung, S. 2010. *Caenorhabditis elegans* swimming in a saturated particulate system. *Phys. Fluids.* 22:031903.
15. Berri, S., J. H. Boyle, …, N. Cohen. 2009. Forward locomotion of the nematode *C. elegans* is achieved through modulation of a single gait. *HFSP J.* 3:186–193.
16. Korta, J., D. A. Clark, …, A. D. Samuel. 2007. Mechanosensation and mechanical load modulate the locomotory gait of swimming *C. elegans*. *J. Exp. Biol.* 210:2383–2389.
17. Fang-Yen, C., M. Wyart, …, A. D. Samuel. 2010. Biomechanical analysis of gait adaptation in the nematode *Caenorhabditis elegans*. *Proc. Natl. Acad. Sci. USA.* 107:20323–20328.
18. Shen, X. N., and P. E. Arratia. 2011. Undulatory swimming in viscoelastic fluids. *Phys. Rev. Lett.* 106:208101.
19. Sznitman, J., X. Shen, …, P. E. Arratia. 2010. Propulsive force measurements and flow behavior of undulatory swimmers at low Reynolds number. *Phys. Fluids.* 22:121901.
20. Pierce-Shimomura, J. T., B. L. Chen, …, S. L. McIntire. 2008. Genetic analysis of crawling and swimming locomotory patterns in *C. elegans*. *Proc. Natl. Acad. Sci. USA.* 105:20982–20987.
21. Mesce, K. A., and J. T. Pierce-Shimomura. 2010. Shared strategies for behavioral switching: understanding how locomotor patterns are turned on and off. *Front. Behav. Neurosci.* 4:49.
22. Vidal-Gadea, A., S. Topper, …, J. T. Pierce-Shimomura. 2011. *Caenorhabditis elegans* selects distinct crawling and swimming gaits via dopamine and serotonin. *Proc. Natl. Acad. Sci. USA.* 108:17504–17509.
23. Boyle, J., S. Berri, …, N. Cohen. 2011. Gait modulation in *C. elegans*: it's not a choice, it's a reflex! *Front. Behav. Neurosci.* 5:10.
24. Sauvage, P., M. Argentina, …, J. M. Di Meglio. 2011. An elasto-hydrodynamical model of friction for the locomotion of *Caenorhabditis elegans*. *J. Biomech.* 44:1117–1122.
25. Nayar, V. T., J. D. Weiland, …, A. M. Hodge. 2012. Elastic and viscoelastic characterization of agar. *J. Mech. Behav. Biomed. Mater.* 70: 60–68.
26. Stiernagle, T. 2006. Maintenance of *C. elegans*. *In* WormBook. The *C. elegans* Research Community. The *C. elegans* Research Community, WormBook, doi/10.1895/wormbook.1.101.1.
27. Ghosh, R., and S. W. Emmons. 2008. Episodic swimming behavior in the nematode *C. elegans*. *J. Exp. Biol.* 211:3703–3711.
28. Abràmoff, M., and P. Magalhães. 2004. Image processing with ImageJ. *Biophot. Intl.* 11:36–42.
29. Eaton, J. W., D. Bateman, and S. Hauberg. 2009. GNU Octave Manual. Network Theory, Bristol, UK.
30. Stephens, G. J., B. Johnson-Kerner, …, W. S. Ryu. 2008. Dimensionality and dynamics in the behavior of *C. elegans*. *PLOS Comput. Biol.* 4:e1000028.
31. Chalfie, M., and J. Sulston. 1981. Developmental genetics of the mechanosensory neurons of *Caenorhabditis elegans*. *Dev. Biol.* 82: 358–370.
32. Li, W., Z. Feng, …, X. Z. Xu. 2006. A *C. elegans* stretch receptor neuron revealed by a mechanosensitive TRP channel homologue. *Nature.* 440:684–687.
33. Wormbase. http://www.wormbase.org.
34. O'Hagan, R., M. Chalfie, and M. B. Goodman. 2005. The MEC-4 DEG/ENaC channel of *Caenorhabditis elegans* touch receptor neurons transduces mechanical signals. *Nat. Neurosci.* 8:43–50.
35. O'Hagan, R., and M. Chalfie. 2006. Mechanosensation in *Caenorhabditis elegans*. *Int. Rev. Neurobiol.* 69:169–203.

36. Park, S., H. Hwang, …, W. S. Ryu. 2008. Enhanced *Caenorhabditis elegans* locomotion in a structured microfluidic environment. *PLoS ONE.* 3:e2550.

37. Kang, L., J. Gao, …, X. Z. Xu. 2010. *C. elegans* TRP family protein TRP-4 is a pore-forming subunit of a native mechanotransduction channel. *Neuron.* 67:381–391.

38. Tavernarakis, N., W. Shreffler, …, M. Driscoll. 1997. *unc-8*, a DEG/ENaC family member, encodes a subunit of a candidate mechanically gated channel that modulates *C. elegans* locomotion. *Neuron.* 18: 107–119.

39. Sznitman, J., P. K. Purohit, …, P. E. Arratia. 2010. Material properties of *Caenorhabditis elegans* swimming at low Reynolds number. *Biophys. J.* 98:617–626.

40. Niebur, E., and P. Erdös. 1991. Theory of the locomotion of nematodes: dynamics of undulatory progression on a surface. *Biophys. J.* 60: 1132–1146.

41. Bryden, J., and N. Cohen. 2008. Neural control of *Caenorhabditis elegans* forward locomotion: the role of sensory feedback. *Biol. Cybern.* 98:339–351.

42. Karbowski, J., G. Schindelman, …, P. W. Sternberg. 2008. Systems level circuit model of *C. elegans* undulatory locomotion: mathematical modeling and molecular genetics. *J. Comput. Neurosci.* 24:253–276.